Kidney International, Vol. 45 (1994), pp. 1510–1521

EGF and TGF-α in the human kidney: Identification of octopal cells in the collecting duct

ETIENNE J. NOUWEN and MARC E. DE BROE

Department Nephrology, University of Antwerp, Antwerp, Belgium

EGF and TGF-α in the human kidney: Identification of octopal cells in the collecting duct. Epidermal growth factor (EGF) and transforming growth factor-alpha (TGF-α) are well-known mitogens expressed in the kidney. Their human renal cell origin has not been conclusively identified. The distribution of EGF and TGF-α was investigated immunohistochemically in the adult human kidney in comparison with the monkey and rodent kidney. In humans, as in the monkey, two variants of EGF immunoreactivity were detected. One was present along the apical cell surfaces and diffusely in the cytoplasm of the thick ascending limb (TAL), co-localizing with Tamm-Horsfall protein, and in the distal convoluted tubule (DCT). The other occurred as overall membranous staining in the connecting tubule and cortical collecting duct (CD), and mainly as basal staining in the rest of the CD. The EGF stained cells in the cortical and outer medullary CD reached a diameter of 40 μ and were identified as intercalated or dark cells; they displayed a peculiar octopus-like shape, bearing long lateral extensions that stretched underneath and between 20 surrounding smaller negative cells. Cytoplasmic TGF-α staining appeared in the DCT and decreased further on. In conclusion: (1) the normal human distal nephron displayed EGF and TGF-α immunoreactivity in a partly complementary segmental and subcellular distribution pattern, partly differing from that in rodents. (2) EGF immunostaining revealed the presence of long lateral projections on CD intercalated cells; this peculiar morphology suggests a modulatory role within the CD epithelium, possibly involving the EGF immunoreactivity on their surface.

Since 1938 it has been known that urine of pregnant women contains a substance, urogastrone, that exerts a potent inhibitory effect on gastric acid secretion [1]. In 1975 it was demonstrated that this substance is identical to epidermal growth factor (EGF) [2, 3], which had been discovered thirteen years earlier in extracts from the male mouse submaxillary gland [4]. EGF appears in normal human urine in appreciable amounts [5]; a renal origin of this urinary EGF is suggested by the finding that its expression in the human kidney by far exceeds that in other tissues [6] and by its comparatively low plasma concentration [5]. Transforming growth factor-alpha (TGF-α) could not be detected in human urine in normal conditions [7], although low expression levels have been demonstrated in renal tissue [8].

EGF and TGF-α belong to the family of EGF-like growth factors, together with amphiregulin, vaccinia virus growth factor, and heparin-binding EGF-like growth factor. Not only do they share 40% sequence homology, they are also indistinguishable with respect to the binding to and activation of the same receptor. The human peptides are proteolytic fragments of separate transmembrane precursors of 1,207 [9] and 160 amino acids [10], respectively. Consequently, mature EGF and TGF-α constitute only 5% and 31% of their precursor sequence. Comparison between the urinary levels of mature EGF and the amount of EGF precursor found in the kidney suggests a high precursor turnover [11, 12].

The documented *in vitro* biological effects of EGF and TGF-α on kidney cells are very similar. They both exert a mitogenic activity on several types of cultured renal epithelial cells [13–16] including human kidney epithelial cells [17–19], as well as on mesenchymal cells [20]. They also enhance renal cell differentiation [21, 22]. Such activities are of potential importance during kidney regeneration, but quite unexpectedly it appears that several types of acute renal failure in the rat are accompanied by a dramatic decrease instead of an increase in the renal expression of EGF [23–27]. Furthermore, exogenous EGF has a rather limited beneficial effect on morphological and functional recovery of the kidney [27–30]. As a result, despite the established reputation of EGF as a growth factor *in vitro*, the biological role for the EGF of renal origin *in vivo* is not known. The same holds true for TGF-α.

Identification of the cells producing these biologically important peptides in the kidney constitutes an essential element in the search for their possible biological function within this organ. Conclusive immunohistochemical and *in situ* hybridization data show that the TAL and early DCT are the sites of EGF expression in the rat and mouse nephron [31–33]. In contrast, and although the link between EGF and the human kidney is already 55 years old, available data on the identity of the cells that produce this EGF in the human nephron are still largely inconclusive. Also, the expression of TGF-α in the normal human kidney has not been thoroughly investigated. As a result, current thinking on the role of renal EGF, either as a mitogen or as a modulator of a yet unidentified distal tubular function(s), departs from the existence of an interspecies homology in cellular and subcellular distribution of EGF between rodents and other species [34, 35], but such a homology has not been demonstrated. Therefore, the primary aim of the present study was the identification of the nephron segments and cell types that express EGF and TGF-α in the adult human kidney.

Received for publication October 22, 1993
and in revised form January 14, 1994
Accepted in revised form January 17, 1994

Methods

Tissues

Adult normal human kidney tissue was obtained: (1) from a live 44-year-old female multi-organ donor, whose kidneys were refused for transplantation because of their spotty appearance after perfusion, and (2) at the moment of surgery from patients with renal cancer involving no more than 50% of the affected kidney ($N = 10$) while having no proteinuria and a normal renal function (as determined from the serum creatinine concentration and calculated creatinine clearance according to the Cockcroft-Gault formula including corrections for age and sex [36]). The latter samples were taken at least 5 centimeters removed from the tumor and displayed a normal morphology upon light microscopical examination. One ureter specimen was also investigated. All samples were processed within 15 minutes after removal. Tissues were cut into 1 to 2 mm thick slices, which were fixed during 1.5 hours at room temperature in Formol-calcium fixative [4% formaldehyde (BDH Chemical Ltd, Poole, UK) in 0.1 M sodium cacodylate buffer, pH 7.4, containing 1% $CaCl_2$], and were embedded in low-melting point (49°C) paraffin (BDH Chemical Ltd). Formol-calcium fixed paraffin-embedded kidney tissue from a Java monkey (*Macaca fascicularis*), a Wistar rat, and a mouse were used in comparison. Alternative tissue processing procedures included: (1) snap-freezing of tissue slices between copper blocks cooled in liquid nitrogen, and fixation of air-dried 6-μ cryostat sections in chloroform-aceton (1/1) during five minutes at room temperature; (2) fixation in periodate/lysine/paraformaldehyde (PLP) fixative during four hours at room temperature and embedding in low-melting point paraffin.

Histotopographic terminology

The standard nomenclature and abbreviations for the different kidney structures, as proposed by Kriz and Bankir [37] on behalf of the Renal Commission of the International Union of Physiological Sciences, were used throughout this study. They are: C, cortex; CD, collecting duct; CNT, connecting tubule; DCT, distal convoluted tubule; IM, inner medulla; ISOM, inner stripe of outer medulla; MR, medullary ray; OM, outer medulla; OSOM, outer stripe of outer medulla; PCT, proximal convoluted tubule, also designated as the S1 and S2 segments; PST proximal straight tubule, also called the S3 segment; TAL, thick ascending limb; TL, thin limb.

Identification of nephron segments and particular cell types

The identity of the segments displaying distinct staining patterns for EGF and TGF-α was established from partial nephron reconstructions using a set of 30 consecutive sections, and from tubular profiles in which the transition from one segment to another could be seen. Additional morphological elements of discrimination were the histotopographical localization and the geometry of tubular cross sections. The identity of the segments was further confirmed on adjacent sections by determining the presence or absence of a set of differentiation markers that cover the entire nephron: alkaline phosphatase and gamma-glutamyl transpeptidase for the proximal tubule; Tamm-Horsfall protein (THP) for the TAL; epithelial membrane antigen and peanut agglutinin binding for the entire distal tubule, as described in a previous study [38]. Histochemical staining for carbonic anhydrase enzyme activity was used to identify the intercalated cells in the CD [35].

Immunohistochemical staining

For EGF, six different commercially-available primary antisera or antibodies were compared on cryostat sections and on paraffin sections without or with trypsin pretreatment: (1) an affinity-purified rabbit antiserum against recombinant human EGF (Ab-3; Oncogene Science, Inc., Uniondale, New York, USA) showing no cross reactivity with human TGF-α, diluted 1/100 to 1/1,000; (2) a rabbit antiserum against recombinant human EGF (Ab 1910, Chemicon International, Inc., Temecula, California, USA), diluted 1/100; (3) a mouse monoclonal antibody against human EGF (MAb 144-8, Santa Cruz Biotechnology, Inc., Santa Cruz, California, USA) not cross reacting with human TGF-α, diluted 1/25 to 1/100; (4) a mouse monoclonal antibody against human EGF purified from urine (MAb 126, Chemicon International, Inc.), diluted 1/25 to 1/1,500; (5) a rabbit antiserum directed against mouse EGF (Sigma Chemical Co., St Louis, Missouri, USA, diluted 1/1,500 to 1/6,000; (6) a rabbit antiserum against rat EGF and not cross reacting with rat TGF-α (RIA-grade; Biomedical Technologies Inc., Stoughton, Massachusetts, USA), diluted 1/20 to 1/100. TGF-α was visualized using a mouse monoclonal antibody against human recombinant TGF-α (Ab-2, Oncogene Science), diluted 1/1,500. Tamm-Horsfall protein was localized using a goat antiserum against human THP (Organon Teknika, Durham, North Carolina, USA), diluted 1/30,000. Epithelial membrane antigen was demonstrated using the monoclonal antibodies HMFG1 and HMFG2 directed against human milk fat globulin [38].

Staining was performed on 4-μ paraffin sections of "formol-calcium" or PLP fixed tissue, essentially as described previously [39]. Briefly, sections were mounted on poly-L-lysine (molecular weight > 300,000; Sigma Chemical) coated glass slides, hydrated, and treated for 20 minutes with 0.003% trypsin (type III, 11,250 U/mg, Sigma Chemical) in 10 mM Tris-HCl buffer (pH 7.3) containing 0.9% NaCl and 1 mM $CaCl_2$. After equilibration in Tris-buffered saline containing 0.1% Triton X-100 (TBS) and treatment with normal horse serum (1/5) for 20 minutes, the primary antibodies were applied without washing, and incubation was performed overnight. The sections were then washed and treated with biotinylated affinity-purified horse anti-mouse immunoglobulin serum (Vector Laboratories Inc., Burlingame, California, USA) for 30 minutes followed by the avidin/biotin/peroxidase complex (Vector Laboratories Inc.) for one hour. All dilutions were made in TBS. After extensive washing, peroxidase was revealed either with 0.02% 3-amino-9-ethylcarbazole (Sigma Chemical) and 0.002% H_2O_2 in 20 mM acetate buffer (pH 5.2) containing 9.5% dimethyl sulfoxide, or with 0.5 mg/ml diaminobenzidine and 0.03% H_2O_2 in 0.1 M Tris-HCl buffer (pH 7.6). The sections were counterstained with methyl green or hematoxylin and were mounted in Kaiser's glycerin/gelatin mounting medium or DPX, respectively. For frozen sections, the incubation buffer contained 1% BSA instead of 0.1% Triton X-100, and endogenous biotin binding activity was reduced by successive preincubation with avidin and 0.1 mg/ml biotin. Simultaneous visualization of EGF and TGF-α on the same section was performed by fluorescence microscopy, using an FITC-labeled donkey anti-rabbit IgG

secondary antiserum (Amersham International plc., Amersham, UK) to reveal EGF, and a Texas Red labeled sheep anti-mouse Ig secondary antiserum (Amersham International plc.) to reveal TGF-α. Sections were inspected either by classical fluorescence microscopy or by confocal laser scanning microscopy.

The specificity of the EGF staining was evaluated by adding different amounts (from 20 ng to 20 μg) of human recombinant EGF (Boehringer Mannheim GmbH, Mannheim, Germany), human recombinant TGF-α (Boehringer Mannheim GmbH), or THP from human urine (Chemicon International, Inc.) to 1 μg/ml anti-EGF IgG (Ab-3) during incubation of the sections. Likewise, the specificity of the TGF-α staining was evaluated by preincubating 200 ng/ml of the antibody with 20 ng to 20 μg human recombinant TGF-α or EGF. Negative controls consisted in replacing the primary rabbit antiserum or mouse monoclonal antibody with diluted normal rabbit serum or an irrelevant monoclonal antibody, respectively.

Histochemical staining

Biotinylated peanut agglutinin (E-Y Laboratories, San Mateo, California, USA) was used at 1 μg/ml and binding was revealed using an avidin-biotinylated peroxidase complex and peroxidase staining (vide infra). Alkaline phosphatase enzymatic staining was performed using 0.025% 5-bromo-4-chloro-3-indoxylphosphate-p-toluidine salt (Serva Feinbiochemica GmbH, Heidelberg, Germany) as the substrate and 0.05% nitroblue tetrazolium (Sigma Chemical Co.) as the chromogen, according to Gossrau [40], in 0.1 M Tris-HCl buffer (pH 9.4) to which was added 1 mM $MgCl_2$. Carbonic anhydrase enzyme activity was demonstrated on 6-μ frozen sections of fixed tissue, floating on a solution containing 1.75 mM $CoSO_4$, 53 mM H_2SO_4, 157 mM $NaHCO_3$, 11.7 mM KH_2PO_4, and 10 ppm Tween 20, according to Lönnerholm [41]. Different fixation conditions were compared for carbonic anhydrase histochemistry: (1) formol-calcium (vide supra); (2) 2% formaldehyde plus 0.2% glutaraldehyde in 0.1 M Na-cacodylate, pH 7.4, during one hour; (3) 2% glutaraldehyde in 0.1 M Na-cacodylate, pH 7.4, containing 1% sucrose, during 1 to 24 hours.

Video densitometry

The polarity of EGF and TGF-α staining in individual cells of different distal tubular segments in the human kidney was measured by digital image analysis. The equipment consisted of a Reichert Polyvar microscope, a color video camera (Hitachi VK-C2000E MOS camera), a screen grabbing card (Screen Machine, FAST Electronic GmbH, München, Germany) with frame grabbing software (SM Camera, version 2.52, ProficomP GmbH, Karlsruhe, Germany), and an Apple Macintosh computer (Model II CX). Analysis was performed using a public domain image analysis computer program (Image, version 1.44, NIH). Eight-bit gray scale pixel values were converted to optical densities by linear interpolation from a series of gray-standards, the optical densities of which were determined in a Beckman spectrophotometer. The optical density was measured along a 30-pixel (2.3 μ) wide transept in the middle of the cell, perpendicular to the apical cell surface. All examples for EGF presented in Figure 3 were taken from a single tissue section, to allow comparison of the staining intensity between cell types.

Results

Staining specificity

Of all the anti-EGF antibodies tested, only the polyclonal antiserum Ab-3 from Oncogene Science and monoclonal antibody 144-8 from Santa Cruz Biotechnology yielded strong and consistent staining. Trypsin pretreatment was necessary for both when used on paraffin sections. For Ab-3, addition of 20 ng human recombinant EGF to 1 μg anti-EGF IgG abolished staining in all distal tubular segments beyond the TAL and DCT. In the latter, staining was also reduced at 20 ng, but 200 ng was necessary to completely eliminate it. Since as much as 20 μg THP purified from human urine had no effect on EGF staining, it can be excluded that the more persistent EGF staining in the TAL would be caused by some cross reactivity with THP, that is abundantly expressed in this segment only. Addition of up to 20 μg TGF-α had no effect on EGF staining. Finally, omission of the primary antibody or replacement by diluted normal rabbit serum abolished the staining pattern. Similarly, addition of 20 ng EGF to MAb 144-8 abolished staining in the TAL and DCT.

TGF-α staining was significantly reduced upon addition of 2 μg human recombinant TGF-α and was completely eliminated when 20 μg was used; the same amount of EGF had no effect. In addition, the staining pattern for TGF-α obtained in the rat kidney (data not shown) was identical to that reported by Walker et al [42] based on the same antibody. Omission of the primary antibody or replacement by an irrelevant mouse monoclonal antibody abolished the staining pattern.

Human kidney

All 11 specimens investigated displayed a consistent segmental and subcellular distribution pattern; there was also no difference in either EGF or TGF-α staining between the organ donor specimen and the samples of normal tissue that were taken from tumor-affected kidneys. Figure 1A provides a low magnification overview of the EGF distribution as obtained with Ab-3 on paraffin sections. Comparisons on adjacent sections demonstrated that there is only a limited overlap between EGF and THP staining (Fig. 1B, C). The EGF staining pattern obtained with monoclonal antibody 144-8 was identical to that for Ab-3, except for the absence of staining beyond the DCT. The distribution of EGF (Ab-3), TGF-α, and THP immunoreactivity along the human nephron are summarized in Figure 1D. Details of the subcellular localization of EGF (Ab-3) and TGF-α staining in different distal tubular segments are shown in Figures 2A through H and 3.

Cortex and medullary ray. EGF staining was absent in the PCT, the medullary ray PST, the glomerular tuft, the epithelium of Bowman's capsule, and the tubular interstitium (Fig. 1A, B). In paraffin sections, most of the cells in the TAL were moderately positive with both the polyclonal antiserum Ab-3 and the monoclonal antibody 144-8, displaying staining predominantly on the apical cell surface and also in the cytoplasm (Figs. 1B, 2A, and 3); the basal plasma membrane infoldings were negative. The macula densa was negative. In fact, the segmental and subcellular distribution of staining for Ab-3 and 144-8 was indistinguishable. All TAL cross sections were strongly positive for THP as well (Fig. 1C). The DCT, which started immediately behind the macula densa and extended to 35 to

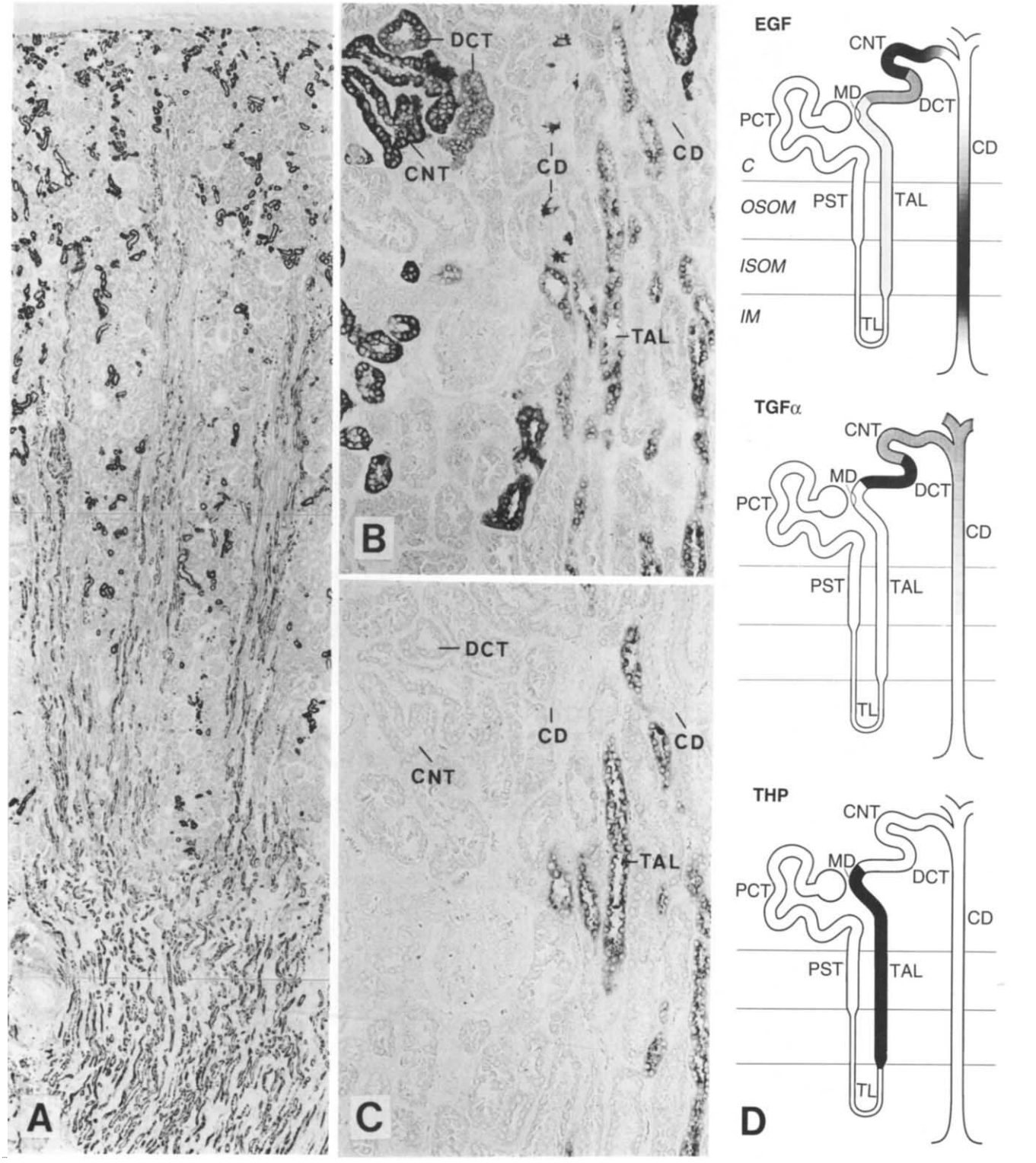

Fig. 1. *Human kidney*. **A.** Low-magnification overview, showing the distribution pattern of EGF immunostaining from the capsula to the ISOM, as obtained with the polyclonal antiserum Ab-3 against human recombinant EGF. **B.** EGF immunoreactivity (Ab-3) in cortical labyrinth and medullary ray; note the octopal cells in the C-CD. **C.** Section adjacent to B, stained for THP. **D.** Schema of the nephron representing the segmental distribution of EGF (Ab-3), TGF-α, and THP immunostaining. (A, × 22; B and C, × 125)

40% of the total length of the distal tubule in the cortical labyrinth (as determined from the frequency of its profiles), displayed moderate EGF staining in all cells, mainly in the cytoplasm but also on the apical cell surface (Figs. 2B and 3). This staining pattern could be confirmed on chloroform-aceton fixed cryostat sections for both Ab-3 and MAb 144-8. In

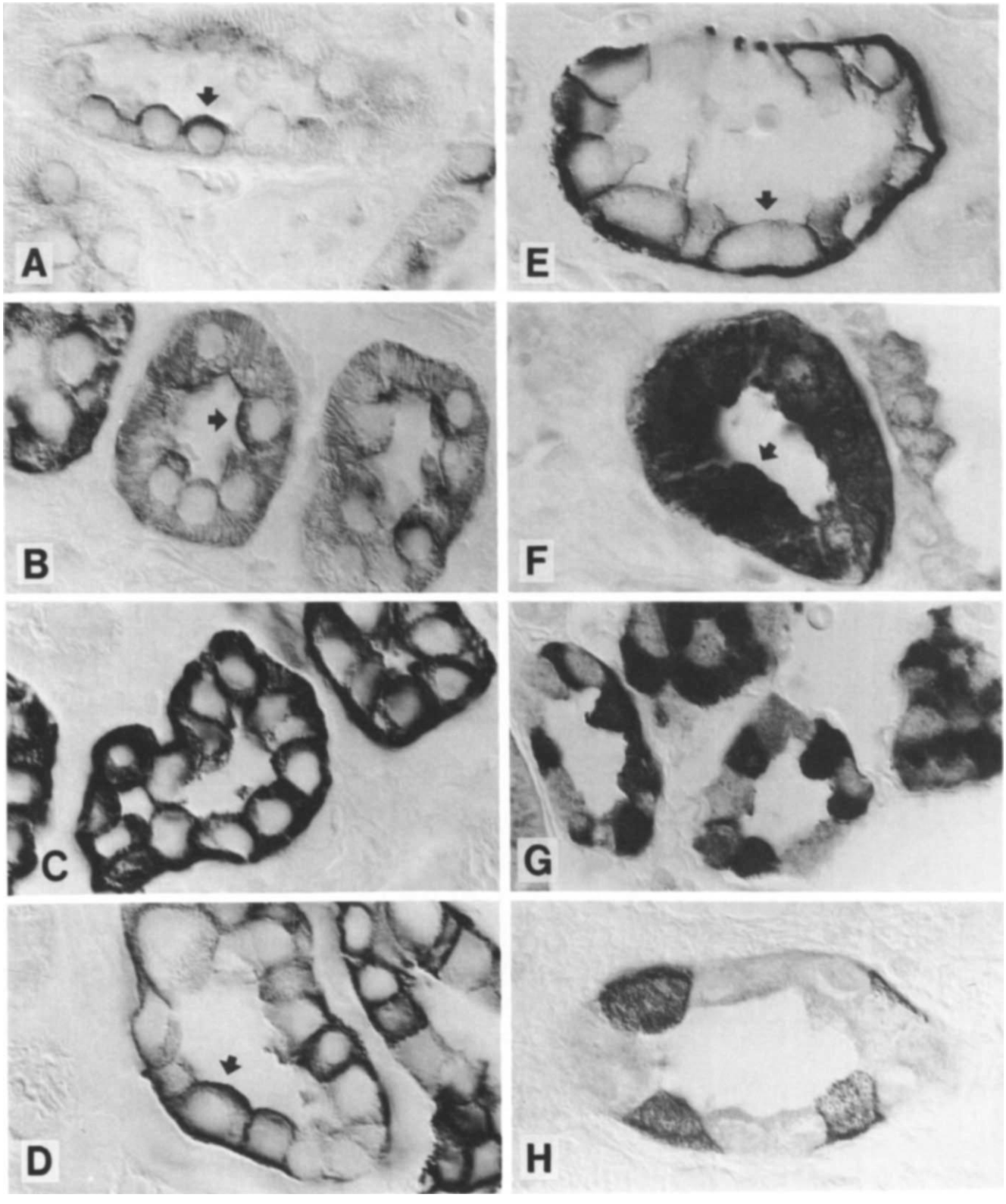

Fig. 2. *EGF (antiserum Ab-3) and TGF-α staining in human kidney.* Arrows indicate cells that were analyzed by video-densitometry to produce the profiles presented in Figure 3. **A.** EGF in ISOM-TAL; **B,** EGF in DCT; **C,** EGF in early CNT; **D,** EGF in late CNT; the number of unstained cells increases towards the C-CD; **E,** EGF in ISOM-CD; **F,** TGF-α in DCT; **G,** TGF-α in CNT; **H,** TGF-α in ISOM-CD: positive cells frequently display intercalated cell morphology. (A through H, × 800)

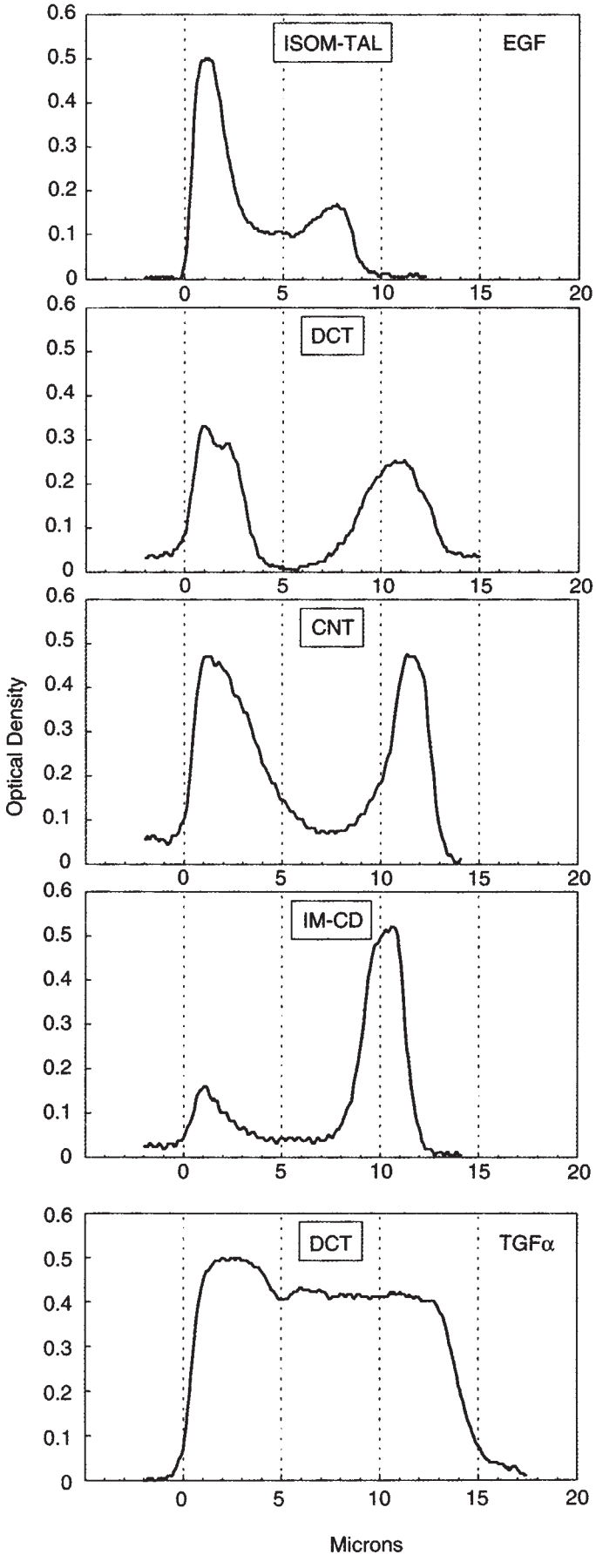

Fig. 3. *Video-densitometric analysis of the subcellular distribution of EGF (Ab-3) and TGF-α staining in individual cells of different distal segments of the human kidney.* All examples for EGF were taken from a single tissue section. The optical density profiles were measured along a 30-pixel wide transept with the background optical density set to zero. The X-axis represents the distance in micron from the luminal towards the basal surface of the cell.

addition, on paraffin sections of formol-calcium or PLP-fixed tissue, Ab-3 revealed strong membranous staining in more distal parts of the nephron. In the remaining 60 to 65% of the distal tubule in the cortical labyrinth, corresponding to the CNT, virtually all cells showed strong staining equally distributed over the entire cell surface (Fig. 2D). Towards the end of the CNT, an increasing number (25 to 50%) of negative cells appeared (Fig. 2E). In the C-CD, the number of positive cells was less than 10% (Fig. 1B); in some cross sections positive cells were even absent. Staining in these CD cells was strong on the basal cell surface, with less intense staining on the lateral and apical cell surfaces. Most of the EGF immunoreactive C-CD cells displayed a specialized morphology, consisting in the presence of long lateral extensions in the basal portion of the cell (vide infra) (Fig. 4).

No TGF-α was seen in the C-TAL, nor in the PCT, glomeruli, or tubular interstitium. Strong and diffuse cytoplasmic staining was observed in most of the cells in the DCT (Figs. 2C and 3). In some cells, staining was stronger at the cell apex. Staining became less intense and more heterogenous in the CNT (Fig. 2F). The C-CD was moderately to weakly positive but a minority of cells presented somewhat stronger staining. Immunoperoxidase staining sometimes suggested the presence of nuclear TGF-α immunoreactivity, but this could not be confirmed upon confocal laser scanning microscopy.

In contrast to EGF staining (Ab-3) in only a small number of C-CD cells, strong carbonic anhydrase histochemical staining appeared in the cytoplasm of virtually all cells lining this segment. The results obtained with the different tissue fixation conditions tested were identical.

Outer medulla. With both Ab-3 and MAb 144-8, EGF staining was seen in the OM-TAL in paraffin as well as in cryosections. Most of the TAL cross sections in the OSOM and ISOM (Fig. 2A) were moderately positive. As in the cortical TAL, staining was localized mainly on the apical cell surface but some positivity was also seen in the cytoplasm; basal plasma membrane infoldings were unstained. Again, Ab-3 revealed the presence of strong EGF-immunoreactivity in the CD in paraffin sections. The OSOM-CD displayed a distribution pattern that was similar to that of the C-CD, with less than 10% of scattered positive cells. Their number increased in the ISOM-CD to approximately 50%, as evidenced by an alternation of positive and negative cells. Like in the C-CD, staining in OSOM- and ISOM-CD cells was particularly strong at the basal cell surface, but the lateral cell surfaces were also stained. Apical staining decreased towards the IM. The PST, TL, and tubular interstitium were negative.

The morphology of the EGF-stained cells (Ab-3) in the OM-CD, and as already mentioned also in the C-CD, was quite peculiar. Some cells had a hat-like profile with a narrow apex and a broad base, bearing long lateral cytoplasmic extensions which passed underneath and between neighboring cells (Fig. 4D, E). When cut tangentially, they displayed a stellate or

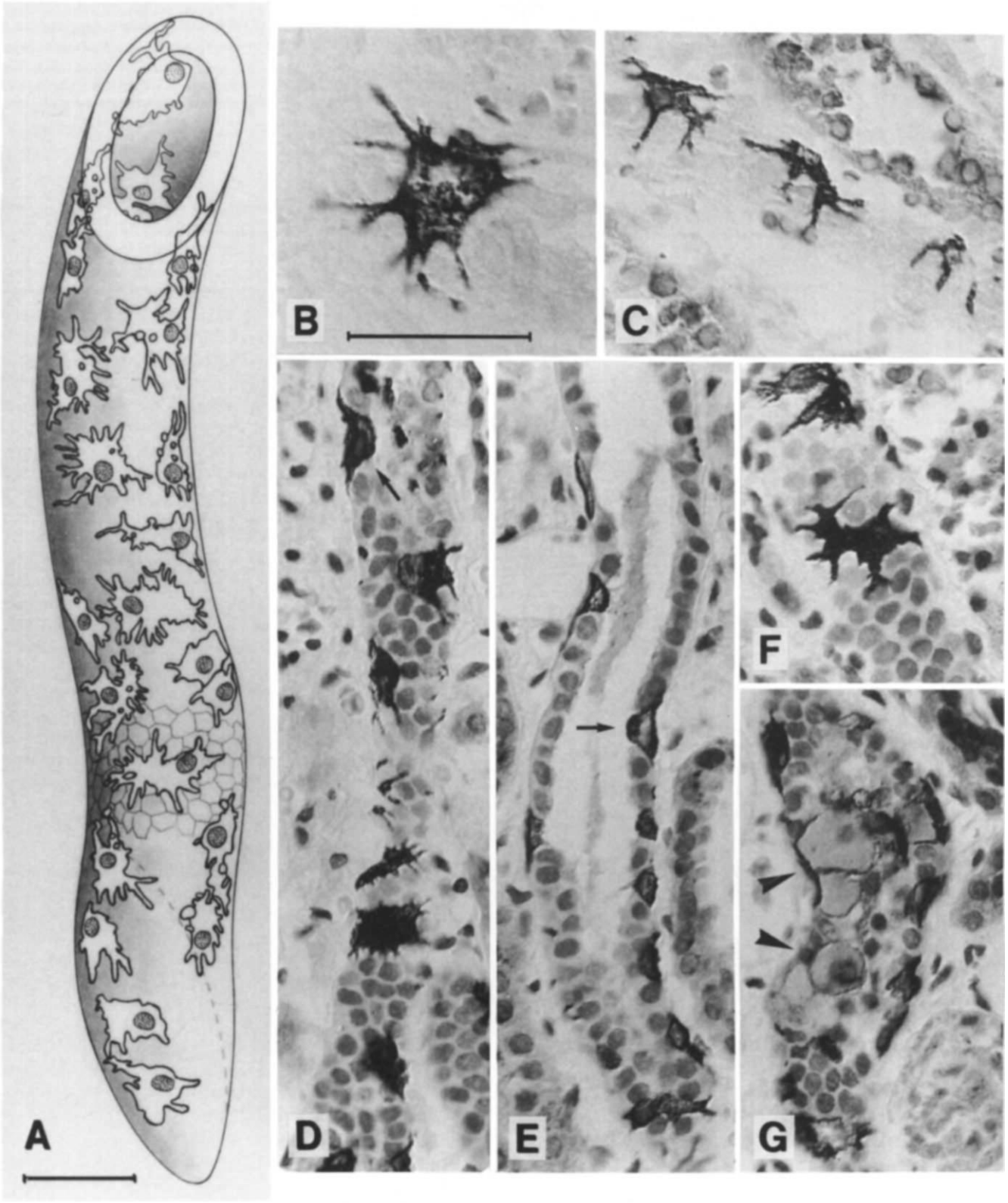

Fig. 4. *EGF staining in octopal cells of the human CD, without (B and C) and with (D–G) hematoxylin nuclear counterstaining to reveal the position of the negative cells in the epithelium.* **A.** Portion of an OSOM-CD as reconstructed from 10 serial sections, illustrating the actual shape and full dimensions of all positively stained intercalated cells visible at one side of the tubule. The negative principal cells are depicted in part of the tubule. B, C, and D. Tangential sections through a C-CD, showing the octopus-like morphology of the large intercalated cells. D and E. Longitudinal section, showing the narrow apex and very broad base of these cells (arrows). F. Tangential sections showing an octopal cell that embraces almost the entire width of the CD. G. Tangential section through positively stained cells without lateral extensions (arrowheads). (A, × 500; B, × 800; C through G, × 500; bar = 40 micron).

dendritic morphology (Fig. 4B, C, D, and F). The general shape of these cells resembled that of an octopus, with its body inserted in the epithelium and reaching the tubular lumen, and its arms extending along the tubular periphery. The lateral projections were shorter in the ISOM-CD and variations in their length were noticed between samples obtained from different individuals. From a set of ten serial sections with a calculated thickness of 5.5 μ, three-dimensional reconstructions were performed for 30 randomly selected EGF-positive cells (Ab-3) in the OSOM-CD (Fig. 4A). This made it possible to trace all extensions belonging to each cell and thus to determine their actual size and shape. While the unstained CD cells had an average width of 6.8 μ ($N = 50$) and a basal area of 36 μ^2, the basal surface of the positively stained stellate cells covered an area of 805 ± 251 μ^2 (mean ± SD; $N = 16$), that is, 22 times larger than the negative cells. The largest one was 38.6 μ in diameter and occupied an area of 1170 μ^2. Those in Figure 4B and C are even slightly larger. This corresponds to about 1/4 of the perimeter of a CD (167 μ). Such cells were never adjacent and via these extensions they were in immediate contact with 21 ± 3 ($N = 7$) negative cells. Other positively stained cells had no cytoplasmic extensions, and their basal area was 217 ± 87 μ^2 ($N = 7$), that is, still 6 × larger than the negative cells (Fig. 4G). They occurred frequently in groups of two or three. The remaining seven cells had an intermediate morphology and basal area (443 ± 173 μ^2). The height of all CD cells was the same (11.4 μ).

TGF-α was absent from the PST, TL, ISOM-TAL, OSOM-TAL, and tubular interstitium. The entire OSOM-CD and ISOM-CD epithelium displayed moderate cytoplasmic staining. In addition, scattered cells within this epithelium showed somewhat stronger cytoplasmic staining (Fig. 2H); their number was considerably smaller than the number of EGF stained cells in these segments. Some of the more positive cells possessed the lateral extensions that were noticed during EGF staining. Comparison on adjacent sections and double immunofluorescent staining revealed that at least some of these cells were also positive for EGF. Like in the medullary rays, carbonic anhydrase staining was strongly positive in the cytoplasm of most OM-CD cells.

Inner medulla. In the IM, there was no EGF staining when MAb 144-8 was used, neither on frozen nor on paraffin sections. Also Ab-3 was unable to detect any EGF immunoreactivity on frozen sections. However, on paraffin sections, staining was seen in the CD. The number of positive cells in the IM-CD1 was between 50 and 75% and decreased to less than 5% in the papillary ducts, with many papillary duct cross-sections containing none or only single positive cells. As in the more proximal CD, staining was localized on the entire cell surface, but was particularly evident at the cell base, where a broad band of staining could be seen. Lateral cellular processes were short or absent. Moderately intense cytoplasmic TGF-α staining was present in the IM-CD_1 and IM-CD_2, but the papillary ducts were negative. Most IM-CD cells were strongly carbonic anhydrase positive, although the number of negative cells increased towards the papillary epithelium.

Papilla and ureter. In paraffin sections, Ab-3 occasionally disclosed membranous EGF staining in a small number (<1%) of round basal cells in the papillary epithelium. The ureter epithelium was always negative. TGF-α staining was absent.

Monkey kidney

The EGF distribution pattern for Ab-3 in formol-calcium fixed paraffin embedded monkey (*Macaca fascicularis*) kidney was identical to the human staining pattern, from the TAL to the papillary epithelium. Moreover, the relative abundance of positive cells in the different segments and the subcellular distribution of staining also was similar, consisting of apical and cytoplasmic staining in the TAL, staining over the entire cell surface in the DCT and CNT, and strong basal staining in the CD. As in the human kidney, the EGF-containing cells of the C-CD and OSOM-CD presented long lateral cellular extensions. TGF-α could not be detected.

Rodent kidney

To confirm the segmental differences between the distribution of EGF immunoreactivity in the primate kidney, as obtained with Ab-3 on paraffin sections, and previous data for the rodent kidney, the staining patterns obtained with an antiserum against either rat, mouse, or human EGF (Ab-3) were compared on adjacent sections from rat and mouse kidney that had been fixed, embedded in paraffin, and stained the same way as the human material. It appeared that the staining patterns for all three antisera were identical in the rat kidney: EGF immunoreactivity was restricted to the TAL and early DCT (data not shown). The subcellular distribution of staining was also identical, as it was strongest in the apical pole of the cells and on the apical cell surface. A similar analogy in staining distribution was obtained for the mouse kidney, although the intensity of staining with the anti-rat and anti-human EGF antisera was low.

Discussion

The immunohistochemical distribution patterns for EGF in the human kidney suggest that there may be two different forms of immunoreactivity present. One is expressed by the TAL and DCT and was detected by both monoclonal antibody 144-8 and by the affinity-purified polyclonal antiserum Ab-3 against human recombinant EGF, in frozen sections and in paraffin sections of formol-calcium or PLP-fixed renal tissue. The other is localized to the CNT and CD and was picked up by Ab-3 in formol-calcium or PLP fixed paraffin embedded material. It is not clear whether this late distal tubular and ductal pool of EGF immunoreactivity corresponds to a conformation of EGF that is masked in native material, or alternatively whether it is associated with the existence of an EGF-related or -resembling epitope in these segments. The non-identity of both pools is further suggested by the observation that the late distal tubular and ductal staining was more rapidly displaced through competition with human recombinant EGF. A distal tubular localization of EGF is in partial agreement with recent *in situ* hybridization data from Lev-Ran et al [43], who demonstrated EGF mRNA in the human DCT and CD, and also in the nuclei of glomerular mesangial cells, but they did not detect any EGF immunoreactivity when using a monoclonal antibody against human EGF. The match between their EGF mRNA localization and our immunohistochemical staining patterns reinforces the validity of the present findings, and it supports a local production of the observed immunoreactivity. Earlier immunohistochemical studies on the human kidney are largely contradictory, as staining was found in each histologic compartment.

Kasselberg et al [44] reported intense staining in extracellular portions of the renal medullary interstitium, increasing towards the papilla and with age. Yoshioka et al [45] described EGF staining in glomerular capillary walls, arterioles, and small arteries, and weak cytoplasmic staining in distal tubules. Poulsen et al [46] observed immunoreactivity in some proximal tubules, whereas Lau, Fowler and Ghosh [47] described cytoplasmic staining in proximal, distal, and collecting ducts, and Kajikawa et al [6] found EGF in tubules which were not identified. In contrast to these disparities for the human kidney, there is agreement on the expression pattern of EGF in the mouse and rat kidney, where several groups have conclusively identified, by immunocytochemistry and *in situ* hybridization, the TAL and early DCT as the only sites of EGF synthesis, while the macula densa was negative [31, 33, 46, 48, 49]. We could confirm this distribution pattern, even with the polyclonal antiserum Ab-3 against human recombinant EGF. Indeed, this antiserum provided a staining pattern in trypsin-pretreated sections from formol-calcium fixed paraffin-embedded rat and mouse kidney that is identical to the staining pattern that has been reported by several other groups for these species, using different antisera and different fixation conditions, including frozen sections. This suggests that the epitope or molecular configuration of EGF occurring in the human kidney beyond the DCT is not present in the rat and mouse kidney. Finally, in the pig, mainly cytoplasmic EGF immunoreactivity was found in the DCT [50]. Hence, it appears that there is indeed interspecies homology in the renal distribution pattern of EGF between humans and rodents, as far as the epitope is concerned that is recognized by antibody 144-8 and Ab-3 in frozen sections and by 144-8 in paraffin sections as well. Interestingly, in the rat and mouse kidney, EGF has an almost perfectly matching colocalization with Tamm-Horsfall protein [51], with which the EGF precursor shares 30% structural homology [52].

The presence of long lateral cell projections, as revealed by Ab-3 on paraffin sections, was an intriguing light microscopical feature of the large EGF stained cells in the adult C-CD and OSOM-CD; they were equally evident in the monkey. These extensions show no resemblance to the pronounced plate-like cell processes that are present between interdigitating DCT cells and that are sparce between CNT cells [35, 53]. However, they fit perfectly the light and electron microscopic descriptions of Möllendorff [54] and Myers et al [55], who mention that the scattered dark or intercalated cells of the human CD bear processes which partially project between adjacent light cells, giving the dark cells a starlike shape. As the intercalated cells constitute a heterogenous population among themselves [35], additional data are needed to establish whether EGF immunostaining is associated with all intercalated cells or only with a specific cellular phenotype. The substantially larger basal pole of the stellate cells in the C-CD and OSOM-CD and their localization partially underneath adjacent cells suggests them to be type B intercalated cells in these segments, whereas in the IM-CD they displayed a type A-like cell morphology. Although carbonic anhydrase expression in the CD is considered as specific for intercalated cells [35, 56], most cells lining the C-CD and OSOM-CD were histochemically positive, which is in agreement with immunohistochemical data from Spicer, Sens and Tashian [57]. Since the number of carbonic anhydrase positive cells largely exceeded the number of EGF stained cells in these segments, it seems that not all intercalated cells contain EGF immunoreactivity, or alternatively that carbonic anhydrase expression in the human CD is not restricted to intercalated cells.

Since the name given to a particular cell type is in general inspired by its most prominent morphological or functional characteristics, one could envisage a new name for the intercalated cell that would better reflect this highly specialized morphology and its potential functional implications. By coincidence, the German name "*Schaltzelle*" can be interpreted as indicating not only the intercalated position of these cells but also a switching or regulatory role. We propose the term "octopal cell," since the long cytoplasmic extensions that irradiate in the basal plane of the cell resemble the arms of an octopus, creeping under and between many surrounding principal cells and probably exerting a modulatory activity upon them. The term could be applicable to other species as well, since the rat intercalated cell shows similar features (unpublished data).

Little or no attention has been attributed during the last 25 years to this unique and highly specialized structural feature of the human intercalated CD cell. The high level of EGF immunostaining on the entire surface of these cells, as described in this study, made their actual shape particularly apparent. Moreover, as it was EGF with its many paracrine activities or an EGF-related epitope that was found on their surface, an extra dimension is added to the potential biological role of these cells. Indeed, these lateral processes, which are remarkably long for epithelial cells, obviously raise the question as to what may be their relevance to the function of the intercalated cell. Since the extensions were often longer than the diameter of a CD principal cell, a single intercalated cell can make direct contact with an average of 21 principal cells that are not necessarily immediately adjacent. In other words, such a cell shape is particularly suited to establish multiple intercellular contacts, reminescent of neurons. Hence, it could be related to a regulatory or coordinating function for the intercalated cell within the CD epithelium, possibly implicating the EGF immunoreactivity on its plasma membrane. CD principal cells are involved in Na^+ reabsorption, K^+ secretion, and ADH-mediated water reabsorption, as evidenced by the polar localization of specific carriers, enzymes, and pumps. Type A intercalated CD cells, on the other hand, are involved in proton secretion, whereas type B intercalated cells secrete bicarbonate and reabsorb chloride [35]. At first glance, none of these intercalated cell functions would benefit from the existence of long cellular processes.

Several reports suggest that EGF may modulate water and electrolyte transport in the collecting duct. A brisk natriuresis and diuresis takes place after infusion of EGF into the sheep renal artery, despite a fall in GRF, suggesting that the effect was tubular and not hemodynamic [58, 59]. When administered basolaterally to rabbit C-CD fragments, very low concentrations of EGF quickly decrease transepithelial voltage and Na-reabsorption [60, 61] and inhibit the hydroosmotic effect of vasopressin [62]. In cultured rat IM-CD, EGF stimulates prostaglandin E_2 synthesis [16], which is also known to inhibit NaCl absorption from the TAL and OM-CD. Our present data indicate that in primates such effects of EGF could be exerted within the CD epithelium, via intercalated cells and their long

lateral cell projections on the neighboring water and salt transporting principal cells with which they are in direct cellular contact, through the production of EGF or a substance containing an EGF-related epitope. Moreover, in analogy to the effect of EGF on gastric mucosa [1], EGF or a related epitope could also modulate the secretion of protons and/or bicarbonate by the intercalated cells in an autocrine way.

We could previously [26] and presently confirm that in the rat, like in the mouse, EGF is predominantly associated with the apical plasma membrane and apical vesicles of the TAL and early DCT [31, 32, 63]. We now present data indicating that predominantly apical (membranous) staining also occurs in the human (and monkey) TAL, and to some extent, in the DCT. In addition, Ab-3 yielded positivity for EGF on the entire cell surface of CNT cells and mainly at the basal cell surface of intercalated cells in the CD. Thus, distal tubular segments displayed differences, not only in the relative intensity of EGF staining and in the number of positive cells, but also in its subcellular localization. A basolateral localization of EGF in the kidney would constitute a new element in the discussion regarding the physiological role(s) of renal EGF. Since an apical localization of EGF is currently considered as the general rule [34] and since EGF receptors, present in the human proximal and distal tubule and the cortical and inner medullary CD [64, 65], have an exclusively basolateral localization at least in the animal kidney [60, 62, 66–69], a straightforward interaction between renal EGF and its receptor is not evident. However, membrane-bound precursor forms of EGF [70] and also of TGF-α [71] may function as ligands to interact with EGF receptors on adjacent cell types. Hence, a juxtacrine interaction would be possible between a basally localized EGF precursor or EGF-related substance, as presently observed in the human and primate CNT and CD, and the EGF receptor.

In addition to EGF, we localized TGF-α immunoreactivity in the distal nephron, in agreement with Mydlo et al [72], who found immunoreactivity in a few distal tubules and CD, although they failed to detect any TGF-α mRNA. Low constitutive levels of TGF-α have also been reported by Gomella et al [8]. A similar ambiguity between TGF-α mRNA and peptide detection exists for the normal rat kidney, where Lee et al [73] detected TGF-α mRNA whereas others did not, although they could demonstrate strong cytoplasmic and nuclear immunoreactivity in some but not all the CD cells, as well as apical staining in the PCT [42]. A possible explanation could be that this renal TGF-α immunoreactivity does not arise from its renal synthesis, but, for example, from filtration. The question also arises as to what may be the biological rationale for the production and/or the presence of both EGF and TGF-α in the normal human distal nephron, with colocalization in many cells of the DCT, CNT, and CD. The two peptides interact with the same receptor and are therefore functionally interchangeable *in vitro* and *in vivo* [19, 74–76]. However, although they are cleavage products of membrane-bound precursor molecules [9, 10], only EGF staining was predominantly membrane-associated whereas TGF-α was exclusively cytoplasmic.

In summary, we presently demonstrated that the two structurally and functionally related growth factors EGF and TGF-α have partially overlapping immunohistochemical distribution patterns in the human kidney. Two pools of EGF staining were detected. One was present along the apical cell surfaces and as diffuse cytoplasmic staining in the TAL and in the DCT. The other variant was present along the rest of the distal nephron and occurred as overall membranous staining in the CNT and as mainly basal staining in the CD. EGF immunostaining further revealed the existence of long lateral cell projections in intercalated CD cells, clearly revealing the octopal morphology of these cells and furthermore suggesting a modulatory role for the intercalated cell within the human CD epithelium.

Acknowledgments

This study was supported by a grant from the Fonds voor Geneeskundig Wetenschappelijk Onderzoek (grant No. 3.0044.92), by a research grant from the University of Antwerp, and by the Belgian programme on Interuniversity Poles of Attraction initiated by the Belgian State, Prime Minister's Office, Science Policy Programming. The authors wish to thank Luc Andries (Department Physiology, Rijksuniversitair Centrum Antwerpen) for performing the confocal laser scanning microscopy and Simonne Dauwe for technical assistance.

Reprint request to Etienne J. Nouwen, Ph.D., Department Nephrology, University of Antwerp, Universiteitsplein 1, B-2610 Wilrijk, Belgium.

References

1. Sandweiss DJ, Saltzstein HC, Farbman A: The prevention of healing of experimental peptic ulcer in Mann-Williamson dogs with the anterior pituitary-like hormone (antuitrin-S). (abstract) *Am J Dig Dis* 5:24, 1938
2. Cohen S, Carpenter G: Human epidermal growth factor: Isolation and chemical and biological properties. *Proc Natl Acad Sci USA* 72:1317–1321, 1975
3. Gregory H: Isolation and structure of urogastrone and its relationship to epidermal growth factor. *Nature* (London) 257:325–328, 1975
4. Cohen S: Isolation of a mouse submaxillary gland protein accelerating incisor eruption and eyelid opening in the newborn animal. *J Biol Chem* 237:1555–1562, 1962
5. Dailey GE, Kraus JW, Orth DN: Homologous radioimmunoassay for human epidermal growth factor (urogastrone). *J Clin Endocrinol Metab* 46:929–936, 1978
6. Kajikawa K, Yasui W, Sumiyoshi H, Yoshida K, Nakayama H, Ayhan A, Yokozaki H, Ito H, Tahara E: Expression of epidermal growth factor in human tissues. *Virchow Arch A Pathol Anat Histopathol* 418:27–32, 1991
7. Stromberg K, Hudgins WR, Orth DN: Urinary TGFs in neoplasia: Immunoreactive TGF-α in the urine of patients with disseminated breast carcinoma. *Biochem Biophys Res Commun* 144:1059–1068, 1987
8. Gomella LG, Sargent ER, Wade TP, Anglard P, Linehan WM, Kasid A: Expression of transforming growth factor α in normal human adult kidney and enhanced expression of transforming growth factors α and beta1 in renal cell carcinoma. *Cancer Res* 49:6972–6975, 1989
9. Bell GI, Fong NM, Stempien MM, Wormsted MA, Caput D, Ku L, Urdea MS, Rall LB, Sanchez-Pescador R: Human epidermal growth factor precursor: cDNA sequence, expression *in vitro* and gene organization. *Nucl Acid Res* 14:8427–8446, 1986
10. Derynck R, Roberts AB, Winkler ME, Chen EY, Goeddel DV: Human transforming growth factor-α: Precursor structure and expression in *E coli*. *Cell* 38:287–297, 1984
11. Breyer JA, Cohen S: The epidermal growth factor precursor from murine kidney membranes. Chemical characterization and biological properties. *J Biol Chem* 265:16564–16570, 1990
12. Perheentupa J, Lakshmanan J, Fisher DA: Urine and kidney EGF: Ontogeny and sex differences in the mouse. *Pediatr Res* 19:428–432, 1985
13. Wilson PD, Horster M: Differential response to hormones of defined distal nephron epithelia in culture. *Am J Physiol* 24:C166–C174, 1983

14. MULLIN JM, MCGINN MT: Epidermal growth factor induced mitogenesis in kidney epithelial cells (LLC-PK1). *Cancer Res* 48:5860–5863, 1988
15. STANTON RC, SEIFTER JL: Epidermal growth factor stimulates growth, Na^+/H^+ exchange and hexose monophosphate shunt activity in rat proximal tubule cells in primary culture. *Am J Physiol* 253:C267–C271, 1988
16. HARRIS RC: Response in rat inner medullary collecting duct to epidermal growth factor. *Am J Physiol* 256:F1117–F1124, 1989
17. WILSON PD: Aberrant epithelial cell growth in autosomal dominant polycystic kidney disease. *Am J Kidney Dis* 17:634–637, 1991
18. WILSON PD, DU J, NORMAN JT: Autocrine, endocrine and paracrine regulation of growth abnormalities in autosomal dominant polycystic kidney disease. *Eur J Cell Biol* 61:131–138, 1993
19. ARGILES A, KRAFT N, OOTAKA T, HUTCHINSON P, ATKINS RC: Epidermal growth factor and transforming growth factor alpha stimulate or inhibit proliferation of a human renal adenocarcinoma cell line depending on cell status: Differentiation of the two pathways by G protein involvement. *Cancer Res* 52:4356–4360, 1992
20. CARPENTER G, COHEN S: Epidermal growth factor. *Annu Rev Biochem* 48:193–216, 1979
21. TAUB M, WANG Y, SZCESNY TM, KLEINMAN HK: Epidermal growth factor or transforming growth factor alpha is required for kidney tubulogenesis in matrigel cultures in serum free medium. *Proc Natl Acad Sci USA* 87:4002–4006, 1990
22. HUMES HD, CIESLINSKI DA: Interaction between growth factors and retinoic acid in the induction of kidney tubulogenesis in tissue culture. *Exp Cell Res* 201:8–15, 1992
23. SAFIRSTEIN R, ZELENT AZ, PRICE PM: Reduced renal prepro-epidermal growth factor mRNA and decreased EGF excretion in ARF. *Kidney Int* 36:810–815, 1989
24. VERSTREPEN WA, NOUWEN EJ, YUE XS, DE BROE ME: Altered growth factor expression during toxic proximal tubular necrosis and regeneration. *Kidney Int* 43:1267–1279, 1993
25. STORCH S, SAGGI S, MEGYESI J, PRICE PM, SAFIRSTEIN R: Ureteral obstruction decreases renal prepro-epidermal growth factor and Tamm-Horsfall expression. *Kidney Int* 42:89–94, 1992
26. NOUWEN EJ, VERSTREPEN WA, BUYSSENS N, ZHU M-Q, DE BROE ME: Hyperplasia, hypertrophy, and phenotypic alterations in the distal nephron after acute proximal tubular injury in the rat. *Lab Invest* (in press)
27. NOUWEN EJ, VERSTREPEN WA, DE BROE ME: Epidermal growth factor in acute renal failure. *Renal Failure* 16:49–60, 1994
28. HUMES HD, CIESLINSKI DA, COÏMBRA TM, MESSANA JM, GALVAO C: Epidermal growth factor enhances renal tubule cell regeneration and repair and accelerates the recovery of renal function in postischemic renal failure. *J Clin Invest* 84:1757–1761, 1989
29. NORMAN J, TSAU Y-K, BACAY A, FINE LG: Epidermal growth factor enhances recovery from ischaemic acute tubular necrosis in the rat: Role of the epidermal growth factor receptor. *Clin Sci* 78:445–450, 1990
30. COÏMBRA TM, CIESLINSKI DA, HUMES HD: Epidermal growth factor accelerates renal repair in mercuric chloride nephrotoxicity. *Am J Physiol* 259:F438–F443, 1990
31. SALIDO EC, LAKSHMANAN J, FISHER DA, SHAPIRO LJ, BARAJAS L: Expression of epidermal growth factor in the rat kidney. An immunocytochemical and *in situ* hybridization study. *Histochemistry* 96:65–72, 1991
32. SALIDO EC, BARAJAS L, LECHAGO J, LABORDE NP, FISHER DA: Immunocytochemical localization of epidermal growth factor in mouse kidney. *J Histochem Cytochem* 34:1155–1160, 1986
33. SALIDO EC, YEN PH, SHAPIRO LJ, FISHER DA, BARAJAS L: *In situ* hybridization of prepro-epidermal growth factor mRNA in the mouse kidney. *Am J Physiol* 256:F632–F638, 1989
34. DANIEL T: Peptide growth factors and the kidney, in *The Kidney: Physiology and Pathophysiology* (vol. 3), edited by SELDIN DW, GIEBISCH G, New York, Raven Press Ltd., 1992, pp. 3135–3155
35. KAISSLING B, KRIZ W: Morphology of the loop of Henle, distal tubule, and collecting duct, in *Handbook of Physiology, Section 8: Renal Physiology*, edited by WINDHAGER EE, Oxford University Press, 1992, pp. 109–167
36. COCKCROFT DW, GAULT MH: Prediction of creatinine clearance from serum creatinine. *Nephron* 16:31–41, 1976
37. KRIZ W, BANKIR L: A standard nomenclature for structures of the kidney. *Kidney Int* 33:1–7, 1988
38. NOUWEN EJ, DAUWE S, VAN DER BIEST I, DE BROE ME: Stage- and segment-specific expression of cell-adhesion molecules N-CAM, A-CAM, and L-CAM in the kidney. *Kidney Int* 44:147–158, 1993
39. NOUWEN EJ, POLLET DE, SCHELSTRAETE JB, EERDEKENS MW, HÄNSCH C, VAN DE VOORDE A, DE BROE ME: Human placental alkaline phosphatase in benign and malignant ovarian neoplasia. *Cancer Res* 45:892–902, 1985
40. GOSSRAU R: Azoindoxylverfahren zum Hydrolasennachweis. IV Zur Eignung verschiedener Diazoniumsalze. *Histochemistry* 57: 323–342, 1978
41. LÖNNERHOLM G: Histochemical demonstration of carbonic anhydrase activity in the human kidney. *Acta Physiol Scand* 88:455–468, 1973
42. WALKER C, EVERITT J, FREED JJ, KNUDSON AG JR, WHITELEY LO: Altered expression of transforming growth factor-α in hereditary rat renal cell carcinoma. *Cancer Res* 51:2973–2978, 1991
43. LEV-RAN A, HWANG DL, BEN-EZRA J, WILLIAMS LE: Origin of urinary epidermal growth factor in humans: Excretion of endogenous EGF and infused [^{131}I]-human EGF and kidney histochemistry. *Clin Exp Pharmacol Physiol* 19:667–673, 1992
44. KASSELBERG AG, ORTH DN, GRAY ME, STAHLMAN MT: Immunocytochemical localization of human epidermal growth factor/urogastrone in several human tissues. *J Histochem Cytochem* 33:315–322, 1985
45. YOSHIOKA K, TAKEMURA T, MURAKAMI K, AKANO N, MATSUBARA K, AYA N, MAKI S: Identification and localization of epidermal growth factor and its receptor in the human glomerulus. *Lab Invest* 63:189–196, 1990
46. POULSEN SS, NEXO E, SKOV OLSEN P, HESS J, KIRKEGAARD P: Immunohistochemical localization of epidermal growth factor in rat and man. *Histochemistry* 85:389–394, 1986
47. LAU JLT, FOWLER JE JR, GHOSH L: Epidermal growth factor in the normal and neoplastic kidney and bladder. *J Urol* 139:170–175, 1988
48. SCOTT J, PATTERSON S, RALL L, BELL GI, CRAWFORD R, PENSHOW J, NIALL H, COGHLAN J: The structure and biosynthesis of epidermal growth factor precursor. *J Cell Sci* (Suppl 3):19–28, 1985
49. JENNISCHE E, ANDERSSON G, HANSSON HA: Epidermal growth factor is expressed by cells in the distal tubules during postnephrectomy renal growth. *Acta Physiol Scand* 129:449–450, 1987
50. VAUGHAN TJ, PASCALL JC, JAMES PS, BROWN KD: Expression of epidermal growth factor and its mRNA in pig kidney, pancreas and other tissues. *Biochem J* 279:315–318, 1991
51. SIKRI KL, FOSTER CL, MACHUGH N, MARSHALL RD: Localisation of Tamm-Horsfall glycoprotein in the human kidney using immunofluorescence and immunoelectron microscopical techniques. *J Anat* 132:597–605, 1981
52. FUKUOKA S, FREEDMAN SD, YU H, SUKHATME VP, SCHEELE GA: GP-2/THP gene family encodes self-binding glycosylphosphatidylinositol-anchored proteins in apical secretory compartments of pancreas and kidney. *Proc Natl Acad Sci USA* 89:1189–1193, 1992
53. TISHER CC, BULGER RE, TRUMP BF: Human renal ultrastructure. III. The distal tubule in healthy individuals. *Lab Invest* 18:655–668, 1966
54. MÖLLENDORFF WV: Der Exkretionsapparat, in *Handbuch der Mikroskopischen Anatomie des Menschen* (vol VII, part I), edited by MÖLLENDORFF WV, Berlin, Springer Verlag, 1930
55. MYERS CE, BULGER RE, TISHER CC, TRUMP BF: Human renal ultrastructure. IV. Collecting duct of healthy individuals. *Lab Invest* 15:1921–1950, 1966
56. LÖNNERHOLM G: Carbonic anhydrase in the monkey kidney. *Histochemistry* 79:195–209, 1983
57. SPICER SS, SENS MA, TASHIAN RE: Immunocytochemical demonstration of carbonic anhydrase in human epithelial cells. *J Histochem Cytochem* 30:864–873, 1982
58. SCOGGINS BA, BUTKUS A, COGHLAN JP, FEI DTW, MCDOUGALL JG, NIALL HD, WALSH JR, WANG X: *In vivo* cardiovascular, renal and endocrine effects of epidermal growth factor in sheep, in *Endocrinology*, edited by LABRIE F, PROULX L, New York, Elsevier, 1984, pp. 573–576
59. GOW CB, WILKINSON M, SILVAPULLE MJ, MOORE GPM: Fluid

balance, electrolyte profiles and plasma parathyroid hormone concentrations in ewes treated with epidermal growth factor. *J Endocrinol* 135:91–101, 1992
60. Vehaskari VM, Hering-Smith KS, Moskowitz DW, Weiner ID, Hamm LL: Effect of epidermal growth factor on sodium transport in the cortical collecting tubule. *Am J Physiol* 256:F803–F809, 1989
61. Hamm LL, Vehaskari VM: Compensatory hypertrophy and adaptation in the cortical collecting duct. *Am J Kidney Dis* 17:647–649, 1991
62. Breyer MD, Jacobson HR, Breyer JA: Epidermal growth factor inhibits the hydroosmotic effect of vasopressin in the isolated perfused rabbit cortical collecting tubule. *J Clin Invest* 82:1313–1320, 1988
63. Salido EC, Fisher DA, Barajas L: Immunoelectron microscopy of epidermal growth factor in mouse kidney. *J Ultrastruct Mol Struct Res* 91:105–113, 1986
64. Gusterson BG, Cowley G, Smith JA, Ozanne B: Cellular localization of human epidermal growth factor receptor. *Cell Biol Int Pep* 8:649–658, 1984
65. Real FX, Rattig WJ, Chesa PG, Melamed MR, Old LJ, Mendelsohn J: Expression of epidermal growth factor in human cultured cells and tissues: Relationship to cell lineage and stage of differentiation. *Cancer Res* 46:4726–4731, 1986
66. Goodyer PR, Kachra Z, Bell C, Rozen R: Renal tubular cells are potential targets for epidermal growth factor. *Am J Physiol* 255:F1191–F1196, 1988
67. Sack EM, Talor Z: High affinity binding sites for epidermal growth factor (EGF) in renal membranes. *Biochem Biophys Res Commun* 154:312–317, 1988
68. Kim DC, Hanano M, Sawada Y, Iga T, Sugiyama Y: Kinetic analysis of clearance of epidermal growth factor in isolated perfused rat kidney. *Am J Physiol* 261:F988–F997, 1991
69. Nielsen S, Nexo E, Christensen EI: Absorption of epidermal growth factor and insulin in rabbit renal proximal tubules. *Am J Physiol* 256:E55–E63, 1989
70. Mroczkowski B, Reich M, Chen K, Bell GI, Cohen S: Recombinant human epidermal growth factor precursor is a glycosylated membrane protein with biological activity. *Mol Cell Biol* 9:2771–2778, 1989
71. Brachmann R, Linquist PB, Nagashima M, Kohr W, Lipari T, Napier M, Derynck R: Transmembrane TGF-α precursors activate EGF/TGF-α receptors. *Cell* 56:691–700, 1989
72. Mydlo JH, Michaeli J, Cordon-Cardo C, Goldenberg AS, Heston WD, Fair WR: Expression of transforming growth factor α and epidermal growth factor receptor messenger RNA in neoplastic and nonneoplastic human kidney tissue. *Cancer Res* 49: 3407–3411, 1989
73. Lee DC, Rose TM, Webb NR, Todaro GJ: Cloning and sequence analysis of a cDNA for rat transforming growth factor-α. *Nature* 313:489–491, 1985
74. Smith JM, Sporn MB, Roberts AB, Derynck R, Winkler ME, Gregory H: Human transforming growth factor-α causes precocious eyelid opening in newborn mice. *Nature* 315:515–516, 1985
75. Rhodes JA, Tam JP, Finke U, Saunders M, Bernanke J, Silen W, Murphy RA: Transforming growth factor α inhibits secretion of gastric acid. *Proc Natl Acad Sci USA* 83:3844–3846, 1986
76. Tam JP: Physiological effects of transforming growth factor in the newborn mouse. *Science* 229:673–675, 1985